Macromolecules

Article

pubs.acs.org/Macromolecules

Nonionic Double and Triple Network Hydrogels of High Mechanical Strength

Aslihan Argun, Volkan Can, Ugur Altun, and Oguz Okay*

Department of Chemistry, Istanbul Technical University, 34469 Maslak, Istanbul, Turkey

Supporting Information

ABSTRACT: Among the hydrogels prepared in recent years, double network (DN) hydrogels exhibit the highest compression strength, toughness, and fracture energies. However, synthesis of DN hydrogels with extraordinary mechanical properties is limited to polyelectrolyte networks, which hinders their widespread applications. Herein, we prepared nonionic DN and triple network (TN) hydrogels based on polyacrylamide (PAAm) and poly(*N*,*N*-dimethylacrylamide) (PDMA) with a high mechanical strength by sequential polymerization reactions. The TN approach is based on the decrease of the translational entropy of the second monomer upon its polymerization in the first network, so that additional solvent (third monomer) can enter into DN hydrogel to assume its new thermodynamic equilibrium. The first network of TN hydrogels comprises chemically cross-linked PAAm or PDMA while the second and third networks are linear polymers. To increase the degree of inhomogeneity of the first network hydrogel, an oligomeric ethylene glycol dimethacrylate was used as a cross-linker in the gel preparation. Depending on the concentration of the first network cross-linker and on the molar ratio of the second and third to the first network units, TN hydrogels contain 89−92% water and exhibit high compressive fracture stresses (up to 19 MPa) and compressive moduli (up to 1.9 MPa).

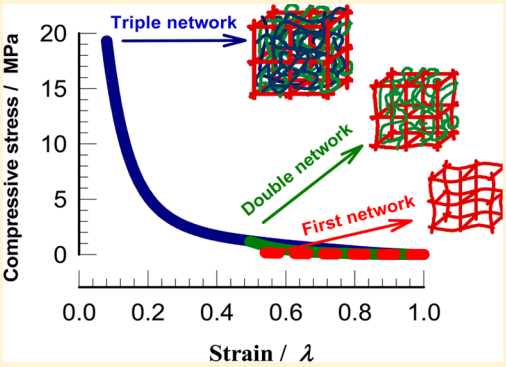

INTRODUCTION

Hydrogels are cross-linked polymers absorbing large quantities of water without dissolving. Softness, smartness, and the capacity to store water make hydrogels unique materials.[1] Although synthetic hydrogels are very similar to biological tissues, they are normally very brittle, which hinders their use in any stress-bearing applications. The poor mechanical performance of chemically cross-linked hydrogels originates from their very low resistance to crack propagation due to the lack of an efficient energy dissipation mechanism in the gel network.[2,3] To obtain a hydrogel with a high degree of toughness, one has to increase the overall energy dissipation along the gel sample by introducing dissipative mechanisms at the molecular level.[4] In recent years, a number of techniques for toughening of gels have been proposed including the double network gels,[5−7] topological gels,[8] nanocomposite hydrogels,[9] cryogels,[10] and supramolecular polymer network hydrogels.[11] Among these materials, double network (DN) hydrogels exhibit the highest and so far unsurpassed compression strength, toughness, and fracture energies.

DN hydrogels described by Gong and co-workers consist of interpenetrating brittle and ductile polymer networks containing 60−90% water.[5] For instance, DN hydrogels made from poly(2-acrylamido-2-methylpropanesulfonic acid) (PAMPS) polyelectrolyte and linear polyacrylamide (PAAm) exhibit exceptional compressive strengths of about 20 MPa and fracture energies in the hundreds of J m^{-2}.[5] Under large strain, the highly cross-linked, brittle first network (PAMPS) breaks up to form many cracks while the second ductile network (PAAm) keeps the gel sample together.[12−15] DN hydrogels are prepared by swelling a highly cross-linked polyelectrolyte first network hydrogel in a solution of a second monomer and then polymerizing the second monomer to form a loosely cross-linked (or linear) second network. Although both networks are sequentially polymerized, some cross-linking between the two networks is possible due to the incomplete polymerization of the first network.[16] Based on the pioneering work of Gong and co-workers,[5] several kinds of DN hydrogels were reported in the literature,[17−22] including the inverse DN hydrogels in that a loosely cross-linked polyelectrolyte network is prepared within the highly cross-linked nonionic network.[23,24]

The mechanical strength of DN hydrogels mainly depends on two experimental parameters:[5] (i) the molar ratio n_{21} of the second to the first network units, which is related to the swelling capacity of the first network hydrogel in the second monomer solution, and (ii) the cross-link density of the first network. Formation of DN hydrogels with extraordinary mechanical performances requires that both the swelling capacity and the cross-link density of the first network must be high. However, since the swelling ratio is inversely proportional to the cross-link density, the DN technique is limited to polyelectrolyte first networks, which hinders its

Received: July 9, 2014
Revised: September 6, 2014
Published: September 12, 2014

   dx.doi.org/10.1021/ma5014176 | Macromolecules 2014, 47, 6430−6440

widespread applications. The requirement of a polyelectrolyte first network for the preparation of high toughness DN hydrogels can be illustrated using the rubber elasticity and equilibrium swelling theories. For instance, assuming phantom network model with tetrafunctional cross-links, the equilibrium swelling ratio of gels is given by[25,26]

$$\ln(1-\varphi_{2,i})+\varphi_{2,i}+\chi_i\varphi_{2,i}^{\ 2}+0.5\nu_{e,i}V_1\varphi_{2,i}^{\ 1/3}\varphi_{2,i}^{0\ 2/3}-f_i\varphi_{2,i}=0 \quad (1a)$$

where $\phi_{2,i}^0$ and $\phi_{2,i}$ are the volume fractions of the cross-linked polymer just after preparation and after equilibrium swelling, respectively, χ_i is the polymer−solvent interaction parameter, $\nu_{e,i}$ is the elastically effective cross-link density of the network, V_1 is the molar volume of solvent, and f_i is the effective charge density in the network. The subindex i in eq 1a equals 1 and 2 for the first and double network hydrogels, respectively. The relative weight ($m_{rel,i}$) and volume ($V_{rel,i}$) swelling ratios with respect to the preparation state of gels are related to the polymer volume fractions $\phi_{2,i}^0$ and $\phi_{2,i}$ by

$$m_{rel,i}\cong V_{rel,i}=\varphi_{2,i}^{\ 0}/\varphi_{2,i} \quad (1b)$$

For the preparation of DN hydrogels, $m_{rel,1}$ of the first network is important, as it determines the n_{21} ratio of the resulting double network. The last term in the left-hand side of eq 1a representing the osmotic pressure of mobile counterions inside the gel is responsible for the high swelling ratio $m_{rel,1}$ of polyelectrolyte first network, i.e., high n_{21} ratio of the corresponding DN hydrogel, even at high cross-link densities $\nu_{e,1}$. For nonionic gels, since this term is zero, $m_{rel,1}$ is close to unity, leading to low n_{21} ratios and thus producing DN's with a poor mechanical performance. To overcome this problem, Gong and co-workers proposed the "molecular stent" approach where linear polyelectrolytes or ionic surfactants are trapped in the first nonionic network to induce gel swelling due to the mobile counterions of these additives.[27]

In the present work, we propose the triple network (TN) approach to create mechanically strong nonionic hydrogels. The TN approach is based on the loss of the translational entropy of a second monomer upon its polymerization within the first network. We have to note that the idea of using the entropy loss on polymerization of a second monomer to permit swelling by a third monomer has very recently been published, admittedly in bulk elastomers rather than hydrogels.[28] The entropy of second monomer, if polymerized in a first network hydrogel, will decrease so that additional solvent (third monomer) can enter into the gel phase to assume its new thermodynamic equilibrium. This means that, assuming the cross-link density of the first network does not change much after DN formation ($\nu_{e,1}\cong\nu_{e,2}\equiv\nu_e$) and both networks consist of the same polymer ($\chi_1=\chi_2\equiv\chi$), DN will swell more than the first network so that triple networks could be prepared. Figure 1 shows calculation results using eqs 1a and 1b, where the swelling ratio $m_{rel,2}$ of nonionic PAAm/PAAm DN hydrogels in water is plotted against the n_{21} ratio (for details see Supporting Information and Figure S1). Calculations are for three first networks formed at $\phi_{2,1}^0$ = 0.10 with different cross-link densities ν_e. The swelling ratios $m_{rel,1}$ of the first network hydrogels are also shown in the figure by symbols. At low values of n_{21}, $m_{rel,2}$ of DN is less than $m_{rel,1}$ of the first network due to the dilution of the double network at the preparation state ($\phi_{2,2}^0<\phi_{2,1}^0$). However, after crossing a critical value of n_{21}, at which the dilution degrees of the first and double networks become equal, $m_{rel,2}$ is larger than $m_{rel,1}$. For instance, DN hydrogel formed at ν_e = 100 mol m^{-3} and n_{21} = 8 exhibits 3-fold larger swelling ratio as compared to its first network hydrogel. Thus, sequential polymerization of the nth monomer solution in $(n-1)$st network would produce multiple-network hydrogels. As will be seen below, this prediction is indeed valid. By sequential polymerization of the second and third monomer solutions in the first and double network hydrogels, respectively, the molar ratio of the second + third polymer to the first polymer units, denoted by $n_{32/1}$, could be increased up to around 60, leading to nonionic TN hydrogels with extraordinary mechanical properties.

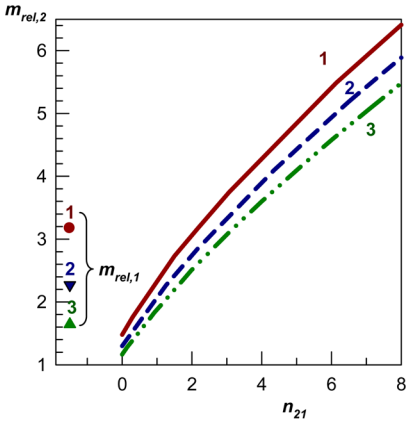

Figure 1. Swelling ratio $m_{rel,2}$ of DN hydrogels in water plotted against n_{21}. Calculations are using eqs 1a and 1b for ν_e = 50 (1), 100 (2), and 200 mol m^{-3} (3). χ = 0.48. V_1 = 18 mL mol^{-1}. $\phi_{2,1}^0$ = 0.10. The swelling ratios $m_{rel,1}$ of first network hydrogels are shown by the symbols.

In the present study, we prepared DN and TN hydrogels consisting of a chemically cross-linked first network and linear polymers as the second and third networks. This paper is organized as follows: Since the first network inhomogeneity seems to affect the mechanical strength of the resulting DN hydrogels,[29,30] we first describe formation conditions of first network PAAm hydrogels with a large degree of inhomogeneity. Polymer gels are known to exhibit an important scattering at low scattering vectors, corresponding to concentration fluctuations at length scale between 10^0 and 10^2 nm.[31,32] Such large-scale concentration fluctuations, which are absent in polymer solutions, are due to the mesoscopic static structures in gels called the spatial gel inhomogeneity.[31−35] The inhomogeneity in gels can be visualized as strongly cross-linked nanogel clusters embedded in a less densely cross-linked environment. A highly inhomogeneous first network with a wide mesh size distribution will absorb larger amounts of the second monomer solution as compared to homogeneous one, leading to higher n_{21} ratios and hence DN hydrogels with a better mechanical performance. As will be seen below, the use of an oligomeric ethylene glycol dimethacrylate as a first network cross-linker instead of the classical cross-linker *N,N′*-methylenebis(acrylamide) enhances the degree of inhomogeneity in PAAm hydrogels. This leads to an increase of n_{21} ratio up to 4.6 and formation of nonionic PAAm/PAAm DN hydrogels with a fracture stress of 5.7 MPa. Swelling these double networks in third monomer solutions further increases the $n_{32/1}$ ratio to 17, producing nonionic PAAm/PAAm/PAAm TN hydrogels containing about 90% water and sustaining up to 10 MPa compressive stresses. In the

dx.doi.org/10.1021/ma5014176 | Macromolecules 2014, 47, 6430−6440

last section, we extend of our approach to the preparation of TN hydrogels based on poly(*N,N*-dimethylacrylamide) (PDMA), a very useful hydrophilic biocompatible polymer with associative properties.[36−38] TN hydrogels based on PDMA possess about 90% water and exhibit a fracture stress of 19 MPa. The excellent mechanical properties of PDMA TN hydrogels are attributed to the hydrophobic interactions between PDMA network chains and the monomer *N,N*-dimethyacrylamide (DMA) in the second monomer solution, leading to $n_{32/1}$ ratios of up to 60.

EXPERIMENTAL PART

Materials. Acrylamide (AAm, Merck), *N,N*-dimethylacrylamide (DMA, Sigma-Aldrich), poly(ethylene glycol) dimethacrylate of molecular weight 550 g/mol (PEG-DM, Aldrich), *N,N′*-methylenebis-(acrylamide) (BAAm, Merck), ammonium persulfate (APS, Sigma-Aldrich), potassium peroxodisulfate (KPS, Fluka), and *N,N,N′,N′*-tetramethylethylenediamine (TEMED, Sigma-Aldrich) were used as received. Stock solutions were prepared by dissolving 0.5 g of APS, 0.1 mL of TEMED, and 0.5 g of KPS separately in 10 mL of distilled water.

Hydrogel Preparation. First network hydrogels were prepared in aqueous solutions of the monomer AAm or DMA and the cross-linker PEG-DM or BAAm at 24 °C in the presence of an APS (4.4 mM)−TEMED (0.025% v/v) redox initiator system. The initial monomer concentration C_1 was fixed at 0.10 g mL^{-1}. The cross-linker content, denoted by mol % of BAAm or PEG-DM with respect to the monomer, was varied over a wide range. Typically, AAm or DMA (1 g) and various amounts of BAAm or PEG-DM were dissolved in water at 24 °C. After bubbling nitrogen, stock solutions of APS (0.20 mL) and TEMED (0.25 mL) were added to obtain a final volume of 10 mL. The solution was then transferred into several plastic syringes of 4.6 mm internal diameter, and the polymerization was conducted for 1 day at 24 °C.

DN hydrogels were prepared by swelling the first network hydrogels in the second AAm or DMA solutions of concentration C_2 between 0.05 and 0.50 g mL^{-1} and polymerizing using 3.7 mM KPS initiator at 60 °C for 24 h. For this purpose, the first network hydrogel just after preparation (about 0.5 g) was immersed in 100 mL of second monomer solution containing AAm or DMA (5−50 g), KPS stock solution (2 mL), and water (98 mL) at 4 °C. Preliminary experiments showed that the polymerization in the external solution did not start at 4 °C during the swelling process of the first network hydrogels, as determined by the turbidity tests conducted by dropping the solutions at various swelling times into acetone or methanol. After reaching the swelling equilibrium at 4 °C, which required 4−6 days, the monomer + initiator solution containing the first network hydrogel was transferred into plastic syringes of 50 mL in volume, and the polymerization was conducted for 1 day at 60 °C. DN hydrogel was then separated by stripping off the external paste-like polymer solution. TN hydrogels were prepared similar to DN hydrogels by swelling DN hydrogels in the third AAm or DMA solution of concentrations C_3 between 0.05 and 0.50 g mL^{-1} and polymerizing using 3.7 mM KPS initiator at 60 °C for 1 day.

Light Scattering Experiments. For the static light scattering (SLS) measurements, gelation reactions for the preparation of first and double network hydrogels were carried out in the light scattering vials. All glassware was kept dust-free by rinsing in hot acetone prior using. The solutions were filtered through membrane filters (pore size = 0.2 μm) directly into the vials. This process was carried out in a dust-free glovebox. All the hydrogels subjected to light scattering measurements were clear and appeared homogeneous to the eye. The light scattering measurements were carried out at 24 °C using a commercial multiangle light scattering DAWN EOS (Wyatt Technologies Corporation) equipped with a vertically polarized 30 mW gallium arsenide laser operating at λ = 690 nm and 18 simultaneously detected scattering angles. The scattered light intensities were recorded from 14.5° to 142.5°, which correspond to the scattering vector q range 3.1 × 10^{-4}−2.3 × 10^{-3} Å^{-1}, where $q = (4\pi n/\lambda)\sin(\theta/2)$, with θ the scattering angle, λ the wavelength of the incident light in vacuum, and n the refractive index of the medium. The light scattering system was calibrated against a toluene standard (Rayleigh ratio at 690 nm = 9.7801 × 10^{-6} cm^{-1}, DAWN EOS software). To obtain the ensemble averaged light scattering intensity of gels, eight cycles of measurements with a small rotation of the vial between each cycle were averaged. The measurements were carried out on first network PAAm hydrogels after preparation and after equilibrium swelling in water as well as on the corresponding DN hydrogels. For the calculation of excess scattering from gels, all the polymerizations reactions were repeated under the same experimental conditions, except that the first network cross-linker was not used. To calculate the excess scattering from swollen first network hydrogels, polymer solutions were diluted to obtain solutions at the same polymer concentration as the swollen gels. Necessary dilution degrees for PAAm solutions were calculated from the equilibrium swelling ratios $V_{rel,1}$ using the equation $V_{sol} = V_{0,sol}V_{rel,1}$, where $V_{0,sol}$ and V_{sol} are the solution volumes before and after dilution with water.[35,39,40] Excess scattering intensity $R_{ex}(q)$, which is a measure of the degree of gel inhomogeneity, was calculated as $R_{ex}(q) = R_{gel}(q) - R_{sol}(q)$, where $R_{gel}(q)$ and $R_{sol}(q)$ are the Rayleigh ratios for gel and polymer solution, respectively.

Figures S2−S4 show $R_{sol}(q)$, $R_{gel}(q)$, and $R_{ex}(q)$ vs scattering vector q plots for the first network hydrogels after preparation and after equilibrium swelling as well as for DN hydrogels. To estimate the amplitude and correlation length of the concentration fluctuations in the hydrogels, the experimental $R_{ex}(q)$ vs q data were fitted to the Debye−Bueche equation:[41−44]

$$R_{ex}(q) = \frac{4\pi K\xi^3\langle\eta^2\rangle}{(1 + q^2\xi^2)^2} \tag{2}$$

where K is the optical constant, $K = 8\pi^2n^2\lambda^{-4}$, ξ is the correlation length of the scatterers, and $\langle\eta^2\rangle$ is the mean-square fluctuation of the refractive index. According to eq 2, the slope and the intercept of $R_{ex}(q)^{-1/2}$ vs q^2 plot (Debye−Bueche plot) give ξ and $\langle\eta^2\rangle$ of a gel sample (Figures S2 and S3).

Swelling and Gel Fraction Measurements. Cylindrical first network, DN, and TN hydrogel samples were immersed in a large excess of water or monomer solutions for at least 6 days by replacing solution every other day to extract any soluble species. The swelling equilibrium was tested by weighing the gel samples. The equilibrium relative weight swelling ratio $m_{rel,i}$, where the subindex i = 1, 2, and 3 stand for the first, double, and triple network hydrogels, respectively, was calculated as

$$m_{rel,i} = \frac{m}{m_0} \tag{3}$$

where m is the mass of the equilibrium swollen gel sample and m_0 is its mass after preparation. From the swelling ratios $m_{rel,1}$ and $m_{rel,2}$ of the first and double network hydrogels in the second and third monomer solutions, respectively, the molar ratio of the network units was estimated using the equations

$$n_{21} = \frac{(m_{rel,1} - 1)C_2}{C_1} \tag{4}$$

$$n_{32/1} = \frac{m_{rel,1}(m_{rel,2} - 1)C_3 + (m_{rel,1} - 1)C_2}{C_1} \tag{5}$$

where n_{21} is the molar ratio of the second to the first network units, $n_{32/1}$ is the molar ratio of the second + third to the first network units, and C_1, C_2, and C_3 are the monomer concentrations (in g mL^{-1}) in the first, second, and third monomer solutions, respectively.[45] The swelling equilibrium of the first network PAAm hydrogels was also tested by measuring the diameter of the gel samples by using an image analyzing system consisting of a microscope (XSZ single Zoom microscope), a CDD digital camera (TK 1381 EG), and a PC with the data analyzing system Image-Pro Plus. The volume swelling ratio $V_{rel,1}$ of the first network hydrogels was calculated as $V_{rel,1} = (D/D_0)^3$, where

dx.doi.org/10.1021/ma5014176 | Macromolecules 2014, 47, 6430−6440

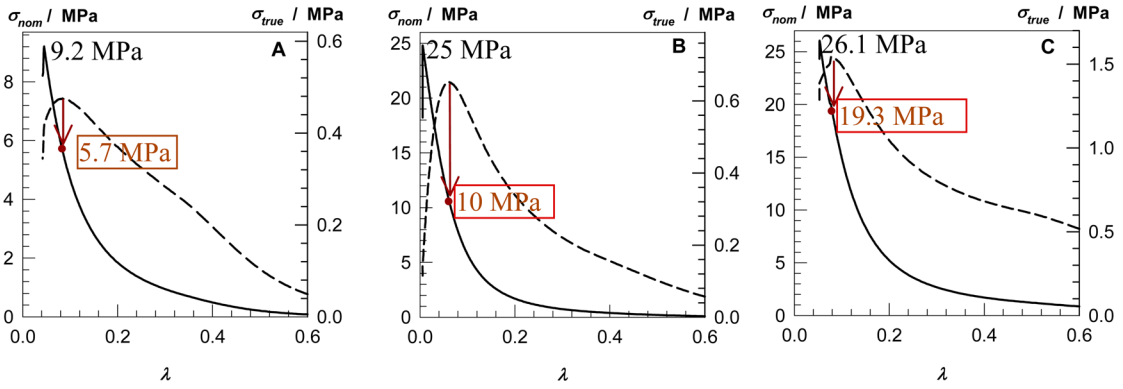

Figure 2. Typical stress−strain curves of hydrogels under compression as the dependences of nominal σ_{nom} (solid curves) and true stresses σ_{true} (dashed curves) on the deformation ratio λ. Red circles are taken as the points of failure in the gel samples. (A) PAAm/PAAm DN hydrogel formed at 4 mol % PEG-DM. n_{21} = 3.6. (B) PAAm/PAAm/PAAm TN hydrogel formed at 4 mol % PEG-DM. n_{21} = 2.6, $n_{32/1}$ = 17. (C) PDMA/PDMA/PDMA TN hydrogel formed at 10 mol % PEG-DM. n_{21} = 4.0, $n_{32/1}$ = 33.

D and D_0 are swollen and initial diameters of the gel sample, respectively.

To determine the gel fraction, the equilibrium swollen gel samples were taken out of water and freeze-dried. The gel fraction W_g, that is, the conversion of monomers to the cross-linked polymer (mass of water-insoluble polymer/initial mass of the monomer in the first, second, and third monomer solutions), was calculated from the masses of dry polymer network and from the comonomer feed. For the first network PAAm hydrogels, the gel fraction W_g was above 0.93 between 0.2 and 3.3 mol % BAAm, while for PEG-DM cross-linker, it decreased from unity to 0.7 as PEG-DM content in the feed is decreased from 4 to 0.3 mol % (Figure S5). W_g was found to be unity for all DN and TN hydrogels formed at various n_{21} and $n_{32/1}$ combinations. Since no cross-linker was included in the second and third monomer solutions, complete incorporation of the linear polymer chains into the first network structure is attributed to the presence of pendant vinyl groups of the first network,[46] to the residual initiator molecules remaining in the hydrogels, and to the self-cross-linking ability of DMA monomer.[47]

Cross-Link Density of the First Network Hydrogels. The average cross-link density ν_e of the first network hydrogels was determined from their stress−strain isotherms measured at 24 °C by using a high precision apparatus previously described.[48] Briefly, a cylindrical first network gel sample just after preparation about 4.6 mm in diameter and 7 mm in length was placed on a digital balance (Sartorius BP221S; readability and reproducibility: 0.1 mg). A load was transmitted vertically to the gel through a rod fitted with a PTFE end-plate. The compressional force acting on the gel was calculated from the reading of the balance. The resulting deformation was measured after 10 s of relaxation by using a digital comparator (IDC type Digimatic Indicator 543-262, Mitutoyo Co.), which was sensitive to displacements of 10^{-3} mm. The measurements were conducted up to about 15% compression. Reversibility of the isotherms was tested by recording the force and the resulting deformation during both force-increasing and force-decreasing processes. The two processes yielded almost identical stress−strain relations. From the repeated measurements, the standard deviations in the modulus value were less than 3%. The sample weight loss during the measurements due to water evaporation was found to be negligible. The elastic modulus G_0 was determined from the slope of linear dependence $\sigma_{nom} = G_0(\lambda - \lambda^{-2})$, where the nominal stress σ_{nom} is the force acting per unit cross-sectional area of the undeformed gel specimen and λ is the deformation ratio (deformed length/initial length). For a tetrafunctional phantom network consisting of Gaussian chains, the elastic modulus G_0 is related to the effective cross-link density ν_e by[26]

$$G_0 = 0.5\nu_e RT\varphi_{2,1}^0 \quad (6)$$

where R and T are in their usual meanings. We have to mention that ν_e calculated using eq 6 is the average value of densely and loosely cross-linked domains of the first network hydrogels.

Mechanical Tests. Uniaxial compression measurements were performed on equilibrium swollen hydrogels at 24 °C on a Zwick Roell test machine using a 500 N load cell. First network gel samples subjected to the mechanical tests were in cylindrical shape of about 5 ± 0.2 mm in diameter and 3.5 ± 0.5 mm in length. DN and TN hydrogels after equilibrium swelling in water were cut into rectangular samples with the dimensions 4 × 4 × 3 mm. Before the test, an initial compressive contact to 0.01 ± 0.002 N was applied to ensure a complete contact between the gel and the plates. Paraffin oil was used as lubricant to reduce friction and adhesion between the plates and the gel surface. The tests were conducted at a constant crosshead speed of 0.3 and 1 mm min^{-1} below and above 15% compression, respectively. Load and displacement data were collected during the experiment. Compressive stress was presented by its nominal σ_{nom} and true values σ_{true}, where the latter is the force per cross-sectional area of the deformed gel specimen, and assuming isotropic deformation during compression, it is given by $\sigma_{true} = \lambda\sigma_{nom}$. The strain is given by the deformation ratio λ or by the biaxial extension ratio λ_{biax} ($=\lambda^{-0.5}$). The Young's modulus E was calculated from the slope of stress−strain curves between 5 and 15% compressions. Cyclic compression tests were conducted at a constant crosshead speed of 1 mm min^{-1} to a maximum compression ratio λ_{max}, followed by retraction to zero force and a waiting time of 1 min, until the next cycle of compression. For reproducibility, at least five samples were measured for each gel, and the results were averaged.

Since compression measurements for gel samples are easier to perform and yield more consistent results than tensile tests, we focused in this study on uniaxial compression tests of DN and TN hydrogels. The fracture stress values are reported as nominal stress to make the results comparable to those of Gong et al.[5] However, we observed that the fracture stress σ_f and fracture strain λ_f obtained from σ_{nom} vs λ curves do not match with those obtained from true stress σ_{true} vs λ curves. For instance, Figures 2A−C show stress−strain curves of three hydrogel samples as the dependences of the nominal σ_{nom} (solid curves) and true stresses σ_{true} (dashed curves) on the deformation ratio λ. The apparent fracture stresses obtained from σ_{nom} vs λ curves are 9.2, 25, and 26.1 MPa at 95, 99, and 95% strains, respectively, while the corresponding σ_{true}−λ plots pass through maxima below these strains. This behavior is likely a result of the hydrogel samples with microscopic cracks still supporting the stress and/or nonisotropic deformation of gel samples under large strain. Therefore, the fracture nominal stress σ_f and strain λ_f at failure were calculated from the maxima in σ_{true}−λ plots, as indicated by the circles in Figure 2. Thus, for the samples in the figures, the fracture stresses σ_f reported are 5.7, 10, and 19.3 MPa at their breaking points.

RESULTS AND DISCUSSION

Elasticity and Inhomogeneity of the First Network PAAm Hydrogels. For the preparation of PAAm first

dx.doi.org/10.1021/ma5014176 | Macromolecules 2014, 47, 6430−6440

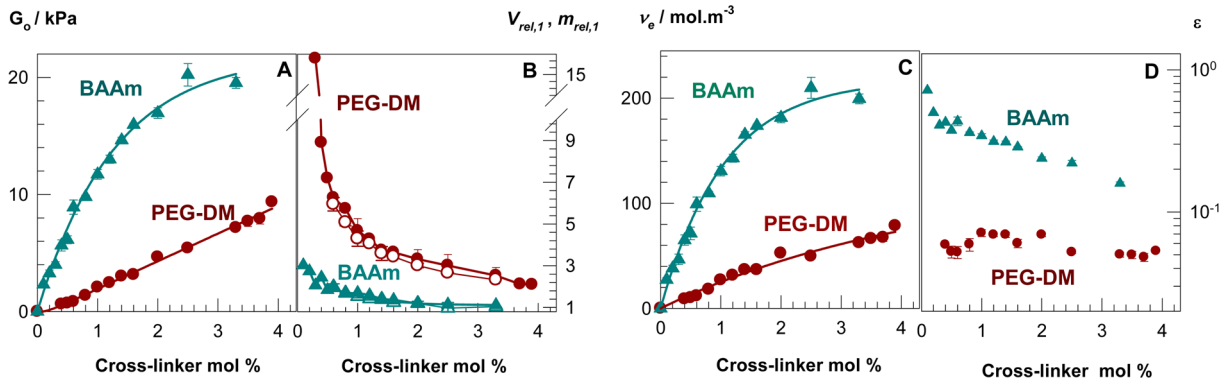

Figure 3. Elastic modulus G_0 (A), swelling ratios $V_{rel,1}$ and $m_{rel,1}$ (B), effective cross-link density ν_e (C), and the cross-linking efficiency ε of first network PAAm hydrogels (D) shown as a function of the cross-linker content. Cross-linker = BAAm (triangles) and PEG-DM (circles). Filled and open symbols in (B) are V_{rel} and m_{rel}, respectively. C_1 = 0.10 g mL^{-1}.

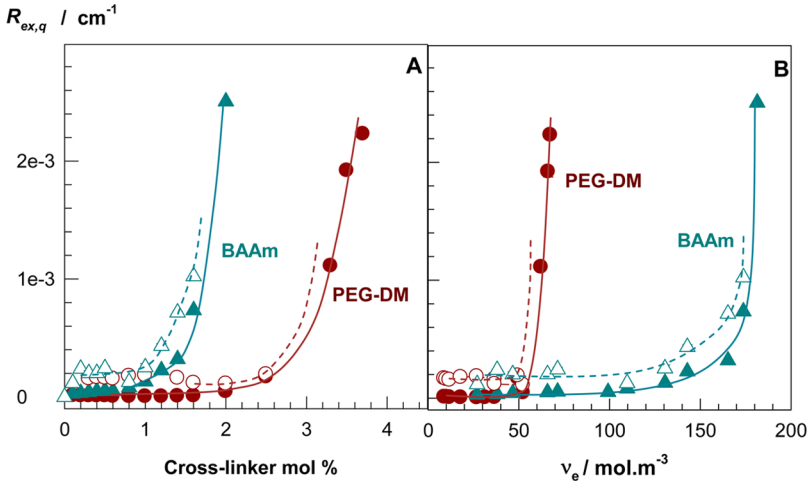

Figure 4. Excess scattering $R_{ex,q}$ measured at θ = 90° shown as a function of cross-linker % and effective cross-link density ν_e of the hydrogels just after their preparation (filled symbols) and after equilibrium swelling in water (open symbols). Cross-linker = BAAm (▲) and PEG-DM (●).

networks, AAm concentration in the feed was fixed at 0.10 g mL^{-1} while the concentrations of the cross-linkers PEG-DM and BAAm were varied. The results from swelling and elasticity tests are plotted in Figures 3A,B. Here, the elastic modulus at the state of gel preparation G_0 (= $E/3$) and the swelling ratios $m_{rel,1}$ and $V_{rel,1}$ of PAAm hydrogels formed using PEG-DM and BAAm cross-linkers are plotted against the cross-linker content. PEG-DM produces hydrogels with a lower modulus of elasticity G_0 and a higher swelling capacity ($V_{rel,1}$ or $m_{rel,1}$) than the classical cross-linker BAAm. Calculation results of the elastically effective cross-link densities ν_e given in Figure 3C reveal that ν_e of the hydrogels generated by PEG-DM is much lower.

Figure 3D shows the efficiency ε of the cross-linkers, that is, the fraction of cross-linker molecules forming elastically effective cross-links plotted against the amount of cross-linker. ε was calculated using the equation $\varepsilon = \nu_e/\nu_{chem}$, where ν_{chem} is the chemical cross-link density, which would result if all cross-linker molecules formed effective cross-links in the hydrogel.[48] The efficiency ε of PEG-DM is around 0.06, indicating that only 6% of PEG-DM in the comonomer feed form elastically effective cross-links and contribute hydrogel elasticity while the rest is wasted in the formation of network defects such as cycles or multiple cross-links.[46] In contrast, ε of BAAm is between 0.2 and 0.8, much larger than that of PEG-DM. The elasticity results thus show that PEG-DM is a less effective cross-linker as compared to BAAm and increases the extent of nonidealities in the gel network.

The degree of inhomogeneity in the first network PAAm hydrogels was investigated by SLS measurements. The gel inhomogeneity was manifested by the excess scattering intensities $R_{ex}(q)$ from PAAm hydrogel over the scattering from a semidilute PAAm solution at the same concentration (Figures S2 and S3). To compare excess scattering of the first network hydrogels, we will focus on the scattering intensity measured at a fixed scattering angle θ of 90° corresponding to q = 1.7 × 10^{-3} Å^{-1}. Figures 4A and 4B show the excess scattering $R_{ex,q}$ at 90° plotted as functions of the cross-linker content and effective cross-link density ν_e, respectively. The data obtained from gels just after preparation and after equilibrium swelling in water are shown by the filled symbols (solid curves) and open symbols (dashed curves), respectively.

A general trend is that $R_{ex,q}$ representing the degree of inhomogeneity in gels remains at a low level up to a critical cross-linker concentration or cross-link density but then rapidly increases. In accord with previous reports,[31,39,40] swelling enhances the degree of inhomogeneity in gels formed by both cross-linkers. At 2.2 mol % BAAm or 4 mol % PEG-DM, the gels became opaque during their preparation, indicating formation of highly cross-linked domains of sizes on the order of the wavelength of light. After swelling, the threshold cross-linker concentration for the appearance of opacity decreases to

dx.doi.org/10.1021/ma5014176 | Macromolecules 2014, 47, 6430−6440

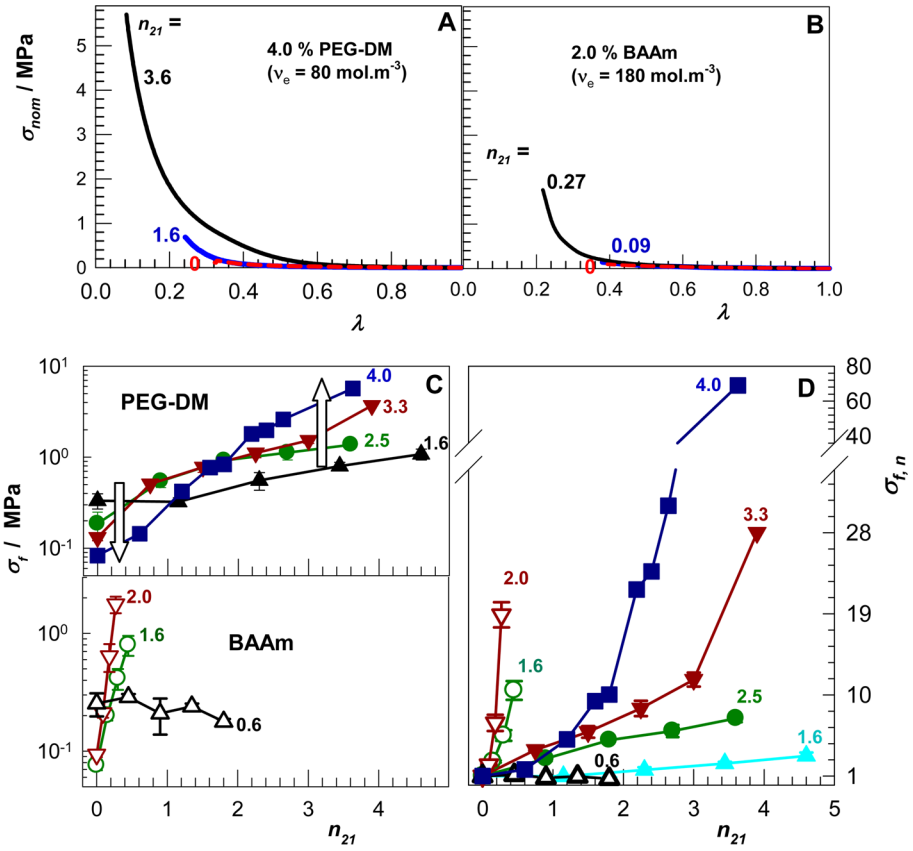

Figure 5. (A, B) Nominal stress σ_{nom} vs deformation ratio λ plots for first network (n_{21} = 0) and DN hydrogels formed using 4.0 mol % PEG-DM (A) and 2.0 mol % BAAm (B). (C) Fracture stress σ_f of DN hydrogels formed using PEG-DM (up) and BAAm (down) plotted against n_{21}. (D) Normalized fracture stress $\sigma_{f,n}$ of DN hydrogels formed using PEG-DM (filled symbols) and BAAm (open symbols) plotted against n_{21}. The amount of the cross-linkers (in mol %) is indicated in (C) and (D).

2.0 and 3.3 mol % for BAAm and PEG-DM, respectively. Figure 4 also shows that the excess scattering from gels rapidly increases after passing 1.4% BAAm or 2.5% PEG-DM, corresponding to a cross-link density ν_e of 150 or 50 mol m^{-3}, respectively. Thus, using BAAm cross-linker, hydrogels with a lesser degree of inhomogeneity could be obtained over a wider range of cross-link densities. This finding is in accord with the elasticity results; as BAAm produces larger number of effective cross-links, the resulting hydrogels are more homogeneous than those formed by PEG-DM cross-linker. Apparently, the cross-linking efficiency of PEG-DM is low (Figure 3D) because it is mainly used to build up highly cross-linked domains instead of yielding a more homogeneous network.

Evaluation of the excess scattering data according to Debye–Bueche function (eq 2) shows that the correlation length of the scatterers ξ in transparent hydrogels is independent of the amount and type of the cross-linker. The data recorded from 52 gel samples both at the preparation and swollen states and at different cross-link densities gave ξ = 18 ± 6 nm (Figure S6). The mean-square fluctuations of the refractive index $\langle\eta^2\rangle$ in gels rapidly increased at ν_e = 50 and 150 mol m^{-3} for PEG-DM and BAAm, respectively (Figure S6). For instance, at a cross-link density ν_e = 78 mol m^{-3}, $\langle\eta^2\rangle$ of the gel formed using PEG-DM is 1.1 × 10^{-5}, while for the gel formed using BAAm is 1 order of magnitude smaller, $\langle\eta^2\rangle$ = 1.8 × 10^{-6}. With the refractive index increment of PAAm in water, dn/dc = 0.163 mL/g,[49] this converts to static concentration fluctuations $\langle\partial c^2\rangle^{1/2}$ = 2.0 × 10^{-2} and 8.2 × 10^{-3} for gels made by PEG-DM and BAAm, respectively. Since the mean polymer concentration in these gels after their preparation is 0.10 g mL^{-1}, the average static concentration fluctuations on a length scale of a few tens of nanometers increase from 8 to 20% by replacing BAAm with PEG-DM as a first network cross-linker. Thus, both the elasticity and inhomogeneity measurements indicate formation more inhomogeneous first network hydrogels using PEG-DM cross-linker as compared to BAAm.

Mechanical Properties of DN Hydrogels. Figures 5A,B show typical compressive stress–strain curves of the first network (n_{21} = 0) and DN hydrogels (n_{21} > 0) formed using PEG-DM (A) and BAAm cross-linkers (B). The highly cross-linked first networks have very low fracture stresses (0.1–0.2 MPa) and fracture strains (60–67%) while increasing ratio n_{21} of the second to the first network improves their mechanical performances. Although the first network formed using PEG-DM is, on average, less cross-linked than that formed using BAAm (ν_e = 80 vs 180 mol m^{-3}), the former network produces a much stronger DN hydrogel (fracture stresses = 5.7 vs 1.8 MPa). This is due to the higher extent of inhomogeneity and thus higher swelling degree of the first networks formed using PEG-DM as compared to BAAm-cross-linked ones (Figure 3B), so that n_{21} could be varied over a wide range, up to 4.6, by changing the second monomer concentration. In Figures 5C,D, the fracture stress σ_f and normalized fracture stress $\sigma_{f,n}$ of DN hydrogels are plotted against n_{21} for various concentration of the first-network cross-linkers. Because of the low swelling degree of BAAm-cross-linked first networks, the n_{21} ratio was limited below 1. Although n_{21} could be increased up to 2 by

dx.doi.org/10.1021/ma5014176 | Macromolecules 2014, 47, 6430–6440

decreasing BAAm content to 0.6 mol %, no improvement in DN properties was observed. As indicated by the arrows in Figure 5C, the mechanical strength of DN hydrogels is inversely proportional to that of their first network hydrogels alone. The lower σ_f of the first network hydrogel, the higher is σ_f of the resulting DN hydrogel. Figure 5D reveals that up to 20-fold and 70-fold improvements in the fracture stress were achieved using BAAm and PEG-DM cross-linkers, respectively. DN hydrogels formed at 4 mol % PEG-DM and n_{21} = 3.6 sustain up to 92% compression and break at a stress of 5.7 MPa.

Visual observations showed that first network hydrogels that were opaque became transparent after formation of DN hydrogels. The most notable improvement in the mechanical properties was observed in DN hydrogels exhibiting an opaque−transparent transition during their formation, i.e., at a cross-linker concentration of around 2 and 4 mol % for BAAm and PEG-DM, respectively. SLS measurements indeed show a significant reduction in the excess scattering intensities $R_{ex}(q)$ of first network hydrogels upon formation of double network structures (Figure S4). Apparently, when AAm is polymerized in the first PAAm network, PAAm chains forming during the reactions concentrate in the less cross-linked (highly swollen) domains of the first network, resulting in the reduction of static concentration fluctuations in DN hydrogels.

Mechanical Properties of TN Hydrogels. As outlined in the Introduction, the equilibrium swelling theory predicts that after crossing a critical n_{21} ratio the swelling capacity of DN hydrogels is higher than that of their first networks alone (Figure 1). This was indeed observed experimentally. Figure 6

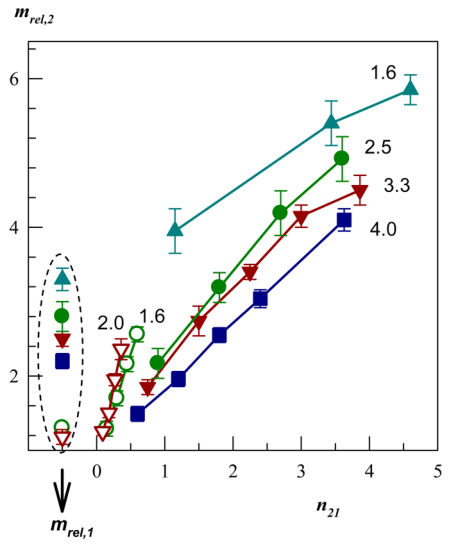

Figure 6. Swelling ratio $m_{rel,2}$ of DN hydrogels prepared using BAAm (open symbols) and PEG-DM (filled symbols) as first network cross-linkers plotted against n_{21}. The cross-linker contents (in mol %) indicated. The swelling ratios $m_{rel,1}$ of the first network hydrogels are also shown.

shows the swelling ratio $m_{rel,2}$ of DN hydrogels formed using BAAm (open symbols) and PEG-DM cross-linkers (filled symbols) plotted against n_{21}. The swelling ratios $m_{rel,1}$ of the first network hydrogels are also shown in the figure. Within the limits of experimental error, both $m_{rel,1}$ and $m_{rel,2}$ are independent of AAm concentration in the monomer solutions used in this study. In accord with the theory, DN's formed above a certain value of n_{21} swell more than their first networks. At $n_{21} \cong 4$, all DN hydrogels formed using PEG-DM cross-linker swell about 1.8-fold larger than the corresponding first networks. This feature opens up the way of preparation TN hydrogels containing larger amount of ductile component (linear PAAm) as compared to DN hydrogels forming in a limited range of n_{21}. We have to mention that, although the increased degree of swelling of DN hydrogels as compared to the first network has, to our knowledge, not been reported before, Gong and co-workers prepared ionic TN hydrogels that exhibit 2-fold higher fracture stress as compared to the corresponding DN hydrogels.[50] This suggests that their ionic DN's also swell more than the first networks.

TN hydrogels were prepared by swelling DN hydrogels in the third AAm solutions containing KPS initiator and polymerizing at 60 °C for 24 h. The molar ratio $n_{32/1}$ of the second + third to the first polymer units was varied by changing AAm concentration in the monomer solution at a fixed n_{21} ratio of DN's. Similar to DN hydrogels, the gel fraction W_g was unity for all TN hydrogels formed at various $n_{32/1}$ ratios. In the swollen state, TN hydrogels contained 88−92% water. The mechanical strength of TN hydrogels formed using BAAm was lower than those formed using PEG-DM due to the lower swelling capacity of their DN's (Figure 6). Therefore, we will only discuss the results obtained using PEG-DM cross-linker.

Figures 7A,B show stress−strain curves of the first network (FN), DN, and TN hydrogels formed using 4 mol % PEG-DM as a first network cross-linker. The fracture stress σ_f of FN hydrogel is 0.15 MPa in both figures, while σ_f of the DN's formed at n_{21} = 1.6 and 3.6 are 0.78 and 5.5 MPa, respectively. TN synthesis starting from these DN's leads to about 6-fold increase in the molar ratio of ductile-to-brittle network components ($n_{32/1}/n_{21}$) and produces hydrogels exhibiting similar fracture stresses (8.4 MPa) and fracture strains (93%). Thus, mechanically weak DN hydrogel formed due to its insufficient n_{21} ratio could be strengthened by incorporation of additional ductile component (linear PAAm) via TN approach. In Figures 7C and 7D, the fracture stresses σ_f of TN hydrogels formed at 3.3 and 4.0 mol % PEG-DM, respectively, are plotted against the $n_{32/1}$ ratio. For comparison, σ_f of FN ($n_{32/1}$ = 0) and DN hydrogels ($n_{32/1}$ = n_{21}, arranged in parallelograms) are indicated. It is seen that the lower the fracture stress of DN hydrogel, the larger the improvement after TN formation. Thus, the relation observed between first network and DN hydrogels is also observable between DN and TN hydrogels. A similar relation was also observed for the Young's modulus E of the hydrogels. The lower E of DN hydrogels, the larger the increase in E upon triple network formation (Figure S7). TN hydrogels with the highest fracture stress (10.2 ± 0.2 MPa) and modulus E (100 ± 8 kPa) were obtained at 4 mol % PEG-DM, n_{21} = 2.6, and $n_{32/1}$ = 17.

The large strain properties of TN hydrogels were investigated by cyclic compression tests conducted up to a strain below the failure. The tests were conducted by compression of gel samples at a constant crosshead speed to a predetermined maximum strain λ_{max}, followed by immediate retraction to zero displacement. After a waiting time of 1 min, the cycles were repeated several times. In Figures 8A,B, four successive loading−unloading cycles of TN hydrogel samples up to a maximum compression of 80% (λ_{max} = 0.2) are shown as the dependence of the nominal stress σ_{nom} on the deformation ratio λ. In all cases, the loading curve of the first compressive cycle is different from the unloading curve, indicating damage in the gel samples and dissipation of energy

dx.doi.org/10.1021/ma5014176 | Macromolecules 2014, 47, 6430−6440

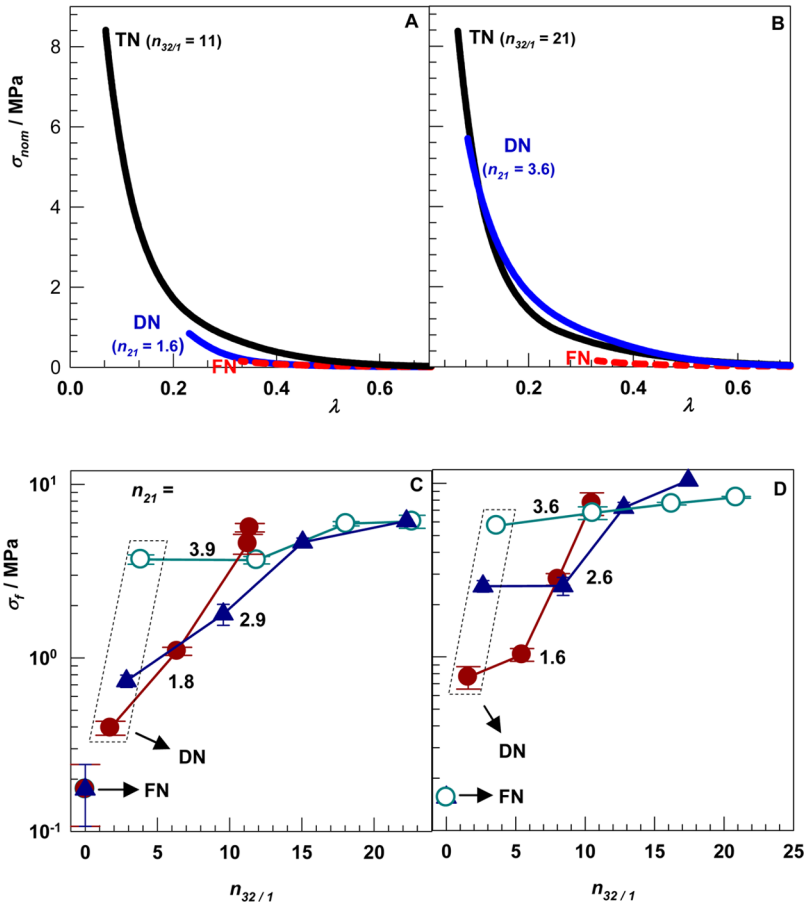

Figure 7. (A, B) Stress σ_{nom} vs deformation ratio λ plots for the first network (FN, red dashed curves), DN, and TN hydrogels. PEG-DM = 4 mol %. n_{21} and $n_{32/1}$ are indicated. (C, D) Fracture stress σ_f of TN hydrogels formed using 3.3 (C) and 4.0 mol % PEG-DM (D) as a first network cross-linker plotted against $n_{32/1}$. For comparison, σ_f of the first network (FN) and DN hydrogels ($n_{32/1} = n_{21}$, arranged in parallelograms) are indicated.

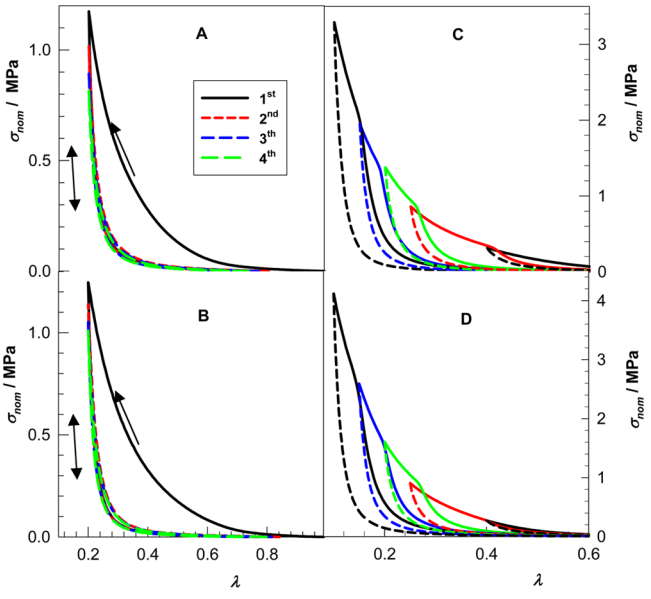

Figure 8. (A, B) Four successive loading/unloading cycles of TN hydrogels up to a maximum compression of 80% (λ_{max} = 0.2). (C, D) Five successive loading/unloading cycles with increasing compression from 60 to 90% (λ_{max} = 0.4 to 0.1). Synthesis parameters of TN hydrogels: n_{21} = 2.7, $n_{32/1}$ = 30 (A, C); n_{21} = 3.6, $n_{32/1}$ = 37 (B, D). PEG-DM = 2.5 mol %.

during the first cycle. However, the second, third, and fourth cycles are almost elastic with a small amount of hysteresis, and they closely follow the path of the first unloading. This clearly indicates the occurrence of an irrecoverable damage to the gel sample during the first cycle. Figures 8C,D show the results of five successive loading/unloading cycles with increasing maximum compression from 60 to 90% (λ_{max} = 0.4 to 0.1). For clarity, loading and unloading curves are shown by the solid and dashed curves, respectively. After the first compressive cycle, each successive loading curve consists of two regions: (1) elastic region that follows the path of the unloading curve of the previous cycle and (2) damage region continuing the loading curve of the previous cycle. The transition from elastic to damage region occurs at the maximum strain of the previous cycle. Thus, due to the irreversible damage done during the previous cycle, additional damage only occurs at a higher maximum strain. The large strain behavior of TN hydrogels reported above is very similar to that of DN hydrogels,[14] where the first cycle hysteresis occurs due to the irreversible fracture of covalent bonds in the highly cross-linked first network. The energy U_{hys} dissipated during the first compression cycles in Figures 8A,B was calculated from the area between the loading and unloading curves. The hysteresis energies U_{hys} (in kJ m^{-3}) were 110 ± 10 and 143 ± 12, respectively, as compared 13 ± 2 and 21 ± 4 for the corresponding DN hydrogels. Thus, the incorporation of third linear polymer into the double network structure leads to 6- to 8-fold increase in energy dissipation. Since the first cycles are irreversible, U_{hys} is associated with the

dx.doi.org/10.1021/ma5014176 | Macromolecules 2014, 47, 6430−6440

number of irreversible broken bonds, i.e., with the number of broken PEG-DM cross-links of the first network. This suggest that the increase in the mechanical strength of TN hydrogels as compared to the corresponding DN hydrogels is due to the increasing amount of the ductile component (third linear PAAm in addition to the second) in triple network structure keeping the gel sample together by breaking more and more chemical cross-links of the first network.

Use of the TN approach to obtain high-strength nonionic hydrogels was also effective for triple network formation using poly(*N*,*N*-dimethylacrylamide) (PDMA), a very useful hydrophilic biocompatible polymer with associative properties.[36−38] Chemically cross-linked PDMA hydrogels generally exhibit rather low mechanical strength due to the lack of an efficient energy dissipation mechanism in the chemically cross-linked network structure. To obtain PDMA triple networks, PEG-DM was used as a first network cross-linker at three different concentrations (4, 6, and 10 mol %). First network hydrogels formed at 4 mol % PEG-DM were transparent while those formed at 6 and 10 mol % were opaque. However, all DN and TN hydrogels starting from these first networks were transparent. At each cross-linker concentration, 4 DN and 16 TN hydrogels were prepared resulting in 48 TN hydrogels with different $n_{32/1}$ ratios. The distinct feature of PDMA hydrogels was their swelling behavior in the monomer (DMA) solutions. While the swelling degree of PAAm hydrogels was independent of AAm concentration in the solution (Figure 6), both $m_{rel,1}$ and $m_{rel,2}$ of PDMA hydrogels increased with DMA concentration in the external solution up to 0.20 g mL^{-1} (Figure S8). This allows higher swelling ratios and hence higher $n_{32/1}$ ratios in TN hydrogels based on PDMA. This additional swelling is attributed to the hydrophobic interactions between DMA monomer in aqueous solutions and PDMA network chains.[36−38]

Figures 9A,B show stress−strain curves of the first network (FN), DN, and TN hydrogels formed at 10 mol % PEG-DM as a first network cross-linker. FN hydrogel breaks at a stress of 0.165 ± 0.05 MPa under 47 ± 4% strain, while DN hydrogels formed at n_{21} = 4.0 and 3.7 sustain at stresses of 1.2 ± 0.2 and 1.7 ± 0.34 MPa, respectively, which are 7−10 times that sustained by FN hydrogel. The fracture stress σ_f of TN hydrogels further increases as the $n_{32/1}$ ratio is increased, and at $n_{32/1}$ = 33, it becomes 19 ± 2 MPa under 91 ± 1% strain (curve 3 in Figure 9A). This fracture stress is more than 110 times that of FN hydrogel. Thus, the TN structure leads to a substantial improvement of the mechanical properties in PDMA hydrogels. As mentioned above, this is due to the increased swelling capacity of DN hydrogels with increasing DMA concentration in the solution.

Figure 10 shows the $n_{32/1}$ dependence of the fracture stresses σ_f and Young's moduli E of 48 TN hydrogels formed at three different concentrations of PEG-DM and at various n_{21} and $n_{32/1}$ combinations. The initial first network hydrogels have fracture stresses 0.21, 0.25, and 0.17 MPa for 4, 6, and 10 mol % PEG-DM, respectively. Increasing the $n_{32/1}$ ratio or increasing concentration of the first network cross-linker also increases the mechanical strength of TN hydrogels. TN hydrogels exhibiting highest fracture stresses (10−19 MPa) and highest Young's moduli (1−2 MPa) were obtained at 10 mol % PEG-DM between $n_{32/1}$ = 10 and 34.

The drastic increase of the modulus E (Figure 10 and Figure S7) upon formation of triple network structures indicates a high degree of physical and chemical connectivity between the

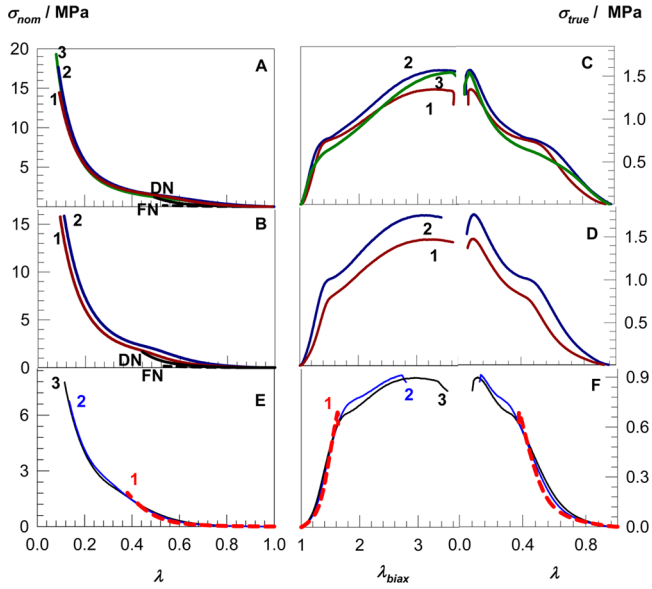

Figure 9. (A, B) σ_{nom} vs λ plots for FN, DN, and TN hydrogels (curves 1−3) formed at 10 mol % PEG-DM as a first network cross-linker. (A) n_{21} = 4.0. $n_{32/1}$ = 20 (1), 27 (2), and 33 (3). (B) n_{21} = 3.7. $n_{32/1}$ = 11 (1), and 17 (2). (C, D) Same curves for TN hydrogels as the dependence of σ_{true} on λ (right) and on the biaxial extension ratio λ_{biax} (left). (E, F) σ_{nom} vs λ (E), σ_{true} vs λ and λ_{biax} plots (F) of TN hydrogels formed at 6 mol % PEG-DM. n_{21} = 1.5. $n_{32/1}$ = 5 (1), 8 (2), and 12 (3).

networks of TN hydrogels.[16,30,51,52] The fact that the gel fraction W_g of both DN and TN hydrogels is unity also supports the existence of interconnected networks in the present hydrogels. Another feature of high strength TN hydrogels based on PDMA is the appearance of a "yielding" type shape in the stress−strain curves at 50−65% compressions (Figures 9A,B). Converting the nominal stress σ_{nom} to its true value σ_{true} and plotting σ_{true} against λ or biaxial extension ratio λ_{biax} make the yielding phenomenon and a plateau region more apparent. This is illustrated in Figures 9C and 9D derived from stress−strain curves in Figures 9A and 9B, respectively. We observed that the yielding appears when $n_{32/1}$ is enough high, that is, when TN hydrogels show a high fracture stress and fracture strain. For instance, Figures 9E,F show stress−strain curves of TN hydrogels formed at 6 mol % PEG-DM and $n_{32/1}$ = 5, 8, and 12, denoted by the curves 1, 2, and 3, respectively. The hydrogels formed at a high $n_{32/1}$ ratio exhibit yielding phenomenon when the true stress σ_{true} reaches to a critical value of 0.7 MPa at λ_{biax} = 1.7 (curves 2 and 3). The yielding region grows up with increasing $n_{32/1}$ ratio, which is responsible for the high fracture stress of TN hydrogels based on PDMA. However, the hydrogel formed at a low $n_{32/1}$ ratio fractures without yielding, and the fracture occurs at σ_{true} = 0.7 MPa and λ_{biax} = 1.6, i.e., at the onset of yielding in high-strength TN hydrogels (curve 1). We may speculate that the yielding behavior of mechanically strong TN hydrogels is related to the appearance of a significant extent of internal fracture under large strain, similar to the necking phenomenon in ionic DN hydrogels observed during uniaxial tensile testing.[12,16,53,54] To analyze internal fracture, TN hydrogels were subjected to cyclic compression tests by successive loading/unloading cycles with increasing maximum strain from 30 to 90%. Similar to TN hydrogels based on PAAm (Figures 7 and 8), each successive loading curve consisted of elastic and damage regions due to

dx.doi.org/10.1021/ma5014176 | *Macromolecules* 2014, 47, 6430−6440

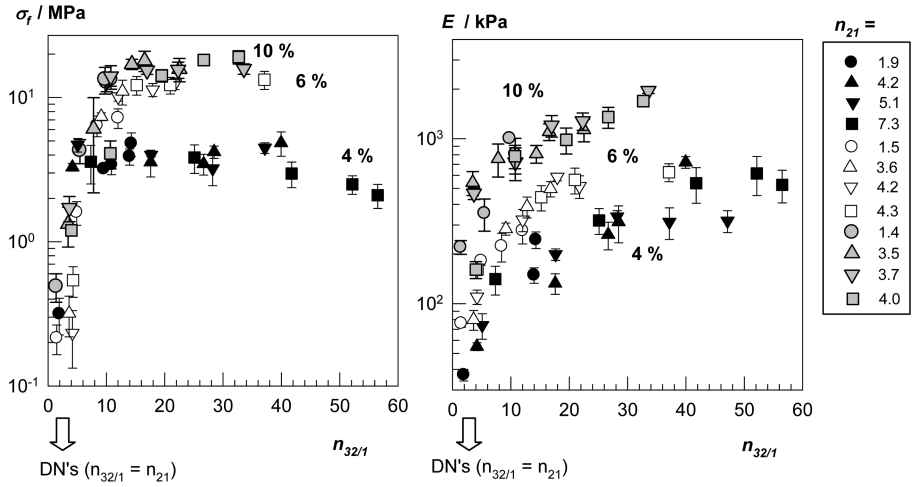

Figure 10. Fracture stress σ_f and Young's modulus E of PDMA TN hydrogels formed using 4 (black symbols), 6 (open symbols), and 10 mol % PEG-DM (gray symbols) plotted against $n_{32/1}$. For comparison, data of DN hydrogels are also shown in the figures.

the irreversible damage done during the previous cycle (Figure S9). The energy U_{hys} dissipated during the cycles increased with increasing maximum strain λ_{max}, and this increase was significant above the yielding region (Figure S9). The small strain modulus E of TN hydrogels decreased during successive loading/unloading cycles as λ_{max} is increased, and after the cycle with λ_{max} = 0.1, it becomes less than the modulus of the first network hydrogel (Figure S10). All these indicate the occurrence of a significant extent of internal fracture in TN hydrogels under large strain conditions which is also responsible for their extraordinary mechanical properties.

CONCLUSIONS

Nonionic PAAm and PDMA hydrogels with extraordinary mechanical properties were obtained by the TN approach, which is based on the decrease of the translational entropy of the second monomer upon its polymerization in the first network, so that additional solvent (third monomer) can enter into the DN gel phase to assume its new thermodynamic equilibrium. The first network comprised chemically cross-linked PAAm or PDMA while the second and third networks were linear polymers. Since the first network inhomogeneity significantly affects the mechanical strength of DN hydrogels, we first described formation conditions of first network PAAm hydrogels with a large degree of inhomogeneity. It was found that the use of PEG-DM as a first network cross-linker instead of the classical cross-linker BAAm increases the degree of inhomogeneity as well as the n_{21} ratio up to 4.6. This leads to the formation of nonionic PAAm/PAAm DN hydrogels with a fracture stress of up to 5.7 MPa. Swelling these double networks in a third monomer solution further increases the $n_{32/1}$ ratio to 17 and produces nonionic PAAm/PAAm/PAAm TN hydrogels containing about 90% water and exhibiting fracture stresses of up to 10 MPa. In the last section, we extend of our approach to the preparation of TN hydrogels based on PDMA, a very useful hydrophilic biocompatible polymer with associative properties. The fracture stress of TN hydrogels based on PDMA further increased due to the hydrophobic interactions between PDMA network chains and DMA monomer in the second monomer solution, leading to $n_{32/1}$ ratios of up to 60. TN hydrogels exhibiting highest fracture stresses (10−19 MPa) and highest Young's moduli (1−2 MPa) were obtained at 10 mol % PEG-DM between $n_{32/1}$ = 10 and 34. High strength TN hydrogels exhibit a "yielding" type shape in their stress−strain curves, which is related to the occurrence of a significant extent of internal fracture in the hydrogels under large strain.

ASSOCIATED CONTENT

Supporting Information

Calculation of the swelling ratios of DN hydrogels; Figure S1, variations of $\phi^0_{2,2}$ and $m_{rel,2}$ of DN hydrogels as functions of n_{21} and C_2; Figures S2−S4, q dependence of the scattering light intensities and DB plots; Figure S5, W_g as a function of cross-linker concentration; Figure S6, ξ and $\langle\eta^2\rangle$ in hydrogels as a function of the cross-link density; Figure S7, Young's modulus of TN hydrogels as a function of $n_{32/1}$; Figure S8, swelling ratio $m_{rel,2}$ of PDMA DN hydrogels plotted against DMA concentration; Figures S9 and S10, loading/unloading cycles, hysteresis energies, and the moduli of TN hydrogels during compression cycles. This material is available free of charge via the Internet at http://pubs.acs.org.

AUTHOR INFORMATION

Corresponding Author

*E-mail okayo@itu.edu.tr (O.O.).

Notes

The authors declare no competing financial interest.

ACKNOWLEDGMENTS

Work was supported by the Scientific and Technical Research Council of Turkey (TUBITAK), KBAG 114Z312. The authors thank Mrs. Emine Yilmaz for the technical assistance during this work. O.O. thanks the Turkish Academy of Sciences (TUBA) for the partial support.

REFERENCES

(1) Okay, O. General properties of hydrogels. In *Hydrogel Sensors and Actuators*; Springer Series on Chemical Sensors and Biosensors; Gerlach, G., Arndt, K.-F., Eds.; Springer: Berlin, 2009; Vol. *6*, pp 1−14.
(2) Ahagon, A.; Gent, A. N. *J. Polym. Sci., Polym. Phys. Ed.* **1975**, *13*, 1903.
(3) Brown, H. R. *Macromolecules* **2007**, *40*, 3815.
(4) Abdurrahmanoglu, S.; Can, V.; Okay, O. *Polymer* **2009**, *50*, 5449.
(5) Gong, J. P.; Katsuyama, Y.; Kurokawa, T.; Osada, Y. *Adv. Mater.* **2003**, *15*, 1155.

(6) Tanaka, Y.; Gong, J. P.; Osada, Y. *Prog. Polym. Sci.* **2005**, *30*, 1.
(7) Haque, M. A.; Kurokawa, T.; Gong, J. P. *Polymer* **2012**, *53*, 1805.
(8) Okumura, Y.; Ito, K. *Adv. Mater.* **2001**, *13*, 485.
(9) Haraguchi, K.; Takehisa, T. *Adv. Mater.* **2002**, *14*, 1120.
(10) Okay, O.; Lozinsky, V. I. *Adv. Polym. Sci.* **2014**, *263*, 103.
(11) Tuncaboylu, D. C.; Sari, M.; Oppermann, W.; Okay, O. *Macromolecules* **2011**, *44*, 4997.
(12) Ahmed, S.; Nakajima, T.; Kurokawa, T.; Haque, M. A.; Gong, J. P. *Polymer* **2014**, *55*, 914.
(13) Nakajima, T.; Fukuda, Y.; Kurokawa, T.; Sakai, T.; Chung, U.; Gong, J. P. *ACS Macro Lett.* **2013**, *2*, 518.
(14) Webber, R. E.; Creton, C.; Brown, H. R.; Gong, J. P. *Macromolecules* **2007**, *40*, 2919.
(15) Nakajima, T.; Kurokawa, T.; Ahmed, S.; Wu, W.; Gong, J. P. *Soft Matter* **2013**, *9*, 1955.
(16) Es-haghi, S. S.; Leonov, A. I.; Weiss, R. A. *Macromolecules* **2013**, *46*, 6203.
(17) Nakayama, A.; Kakugo, A.; Gong, J. P.; Osada, Y.; Takai, M.; Erata, T.; Kawano, S. *Adv. Funct. Mater.* **2004**, *14*, 1124.
(18) Xin, H.; Saricilar, S. Z.; Brown, H. R.; Whitten, P. G.; Spinks, G. M. *Macromolecules* **2013**, *46*, 6613.
(19) Harrass, K.; Kruger, R.; M?ller, M.; Albrecht, K.; Groll, J. *Soft Matter* **2013**, *9*, 2869.
(20) Yasuda, K.; Gong, J. P.; Katsuyama, Y.; Nakayama, A.; Tanabe, Y.; Kondo, E.; Ueno, M.; Osada, Y. *Biomaterials* **2005**, *26*, 4468.
(21) Hu, J.; Kurokawa, T.; Nakajima, T.; Sun, T. L.; Suekama, T.; Wu, Z. L.; Liang, S. M.; Gong, J. P. *Macromolecules* **2012**, *45*, 9445.
(22) Fei, R.; George, J. T.; Park, J.; Means, A. K.; Grunlan, M. A. *Soft Matter* **2013**, *9*, 2912.
(23) Myung, D.; Koh, W.; Ko, J.; Hu, Y.; Carrasco, M.; Noolandi, J.; Ta, C. N.; Frank, C. W. *Polymer* **2007**, *48*, 5376.
(24) Waters, D. J.; Engberg, K.; Parke-Houben, R.; Ta, C. N.; Jackson, A. J.; Toney, M. F.; Frank, C. W. *Macromolecules* **2011**, *44*, 5776.
(25) Flory, P. J. *Principles of Polymer Chemistry*; Cornell University Press: Ithaca, NY, 1953.
(26) Treloar, L. R. G. *The Physics of Rubber Elasticity*; University Press: Oxford, 1975.
(27) Nakajima, T.; Sato, H.; Zhao, Y.; Kawahara, S.; Kurokawa, T.; Sugahara, K.; Gong, J. P. *Adv. Funct. Mater.* **2012**, *22*, 4426.
(28) Ducrot, E.; Chen, Y.; Bulters, M.; Sijbesma, R. P.; Creton, C. *Science* **2014**, *344*, 186.
(29) Na, Y.-H.; Kurokawa, T.; Katsuyama, Y.; Tsukeshiba, H.; Gong, J. P.; Osada, Y.; Okabe, S.; Karino, T.; Shibayama, M. *Macromolecules* **2004**, *37*, 5370.
(30) Huang, M.; Furukawa, H.; Tanaka, Y.; Nakajima, T.; Osada, Y.; Gong, J. P. *Macromolecules* **2007**, *40*, 6658.
(31) Bastide, J.; Candau, S. J. In *Physical Properties of Polymeric Gels*; Cohen Addad, J. P., Ed.; Wiley: New York, 1996; p 143.
(32) Shibayama, M. *Macromol. Chem. Phys.* **1998**, *199*, 1.
(33) Shibayama, M.; Ikkai, F.; Nomura, S. *Macromolecules* **1994**, *27*, 6383.
(34) Lindemann, B.; Schröder, U. P.; Oppermann, W. *Macromolecules* **1997**, *30*, 4073.
(35) Kizilay, M. Y.; Okay, O. *Macromolecules* **2003**, *36*, 6856.
(36) Uemura, Y.; McNulty, J.; Macdonald, P. M. *Macromolecules* **1995**, *28*, 4150.
(37) Peppas, N. A. *Hydrogels in Medicine and Pharmacy*; Wiley: New York, 1987.
(38) Relogio, P.; Martinho, J. M. G.; Farinha, J. P. S. *Macromolecules* **2005**, *38*, 10799.
(39) Kizilay, M. Y.; Okay, O. *Polymer* **2004**, *45*, 2567.
(40) Yazici, I.; Okay, O. *Polymer* **2005**, *46*, 2595.
(41) Debye, P. J. *J. Chem. Phys.* **1959**, *31*, 680.
(42) Bueche, F. *J. Colloid Interface* **1970**, *33*, 61.
(43) Debye, P.; Bueche, A. M. *J. Appl. Phys.* **1949**, *20*, 518.
(44) Soni, V. K.; Stein, R. S. *Macromolecules* **1990**, *23*, 5257.
(45) Equations 4 and 5 neglect the exchange of water in the hydrogel with the external solution and thus only consider monomer solution entering the gel phase during the swelling process to simulate real processes. See e.g.: Kayaman, N.; Okay, O.; Baysal, B. M. *Polym. Gels Networks* **1997**, *5*, 339.
(46) Okay, O.; Kurz, M.; Lutz, K.; Funke, W. *Macromolecules* **1995**, *28*, 2728.
(47) Cipriano, B. H.; Banik, S. J.; Sharma, R.; Rumore, D.; Hwang, W.; Briber, R. M.; Raghavan, S. R. *Macromolecules* **2014**, *47*, 4445.
(48) Gundogan, N.; Melekaslan, D.; Okay, O. *Macromolecules* **2002**, *35*, 5616.
(49) Orakdogen, N.; Okay, O. *J. Appl. Polym. Sci.* **2007**, *103*, 3228.
(50) Kaneko, D.; Tada, T.; Kurokawa, T.; Gong, J. P.; Osada, Y. *Adv. Mater.* **2005**, *17*, 535.
(51) Nakajima, T.; Furukawa, H.; Tanaka, Y.; Kurokawa, T.; Osada, Y.; Gong, J. P. *Macromolecules* **2009**, *42*, 2184.
(52) We have to note that the increase of the modulus E upon formation of TN structures is inconsistent with the assumption of the derivations given in the Supporting Information. However, entropic terms of eq 1a still dominate over the elastic term so that TN hydrogels swell more than their DN hydrogels.
(53) Na, Y.-H.; Tanaka, Y.; Kawauchi, Y.; Furukawa, H.; Sumiyoshi, T.; Gong, J. P.; Osada, Y. *Macromolecules* **2006**, *39*, 4641.
(54) Tanaka, Y.; Kawauchi, Y.; Kurokawa, T.; Furukawa, H.; Okajima, T.; Gong, J. P. *Macromol. Rapid Commun.* **2008**, *29*, 1514.